Relative intensities of gadolinium L X-Rays, induced by proton bombardment at energies between 200 keV to 750 keV

C.E. Canto, O.G. de Lucio, J.G. Morales, and J.C. Pineda
Instituto de Física, Universidad Nacional Autónoma de México
Apartado Postal 20-364 01000, México D.F., México

Recibido el 17 de enero de 2012; aceptado el 3 de febrero de 2012

Relative intensities of Gd characteristic L X-Ray, induced by proton impact have been measured for GdF_3 thin films, as a function of projectile energy and also as a function of a variable defined as the relative velocity of the incoming particle. Results are presented as intensity ratios for L sub-shells and intensity ratios for particular transitions both of them measured with respect to the total number of X-ray photons recorded; in all cases it is possible to show an energy dependence for these intensity ratios. Complementary microanalysis studies (AFM, SEM/EDS) were performed in order to have accurate information on the chemical composition and surface properties of the thin films.

Keywords: PIXE; X-ray lines relative intensity; low energy accelerator physics.

Se midieron las intensidades relativas de rayos X característicos de Gd, inducidos por impacto de protones en películas delgadas de GdF_3, como función de la energía del proyectil y de una variable definida como la velocidad relativa del proyectil. Los resultados se presentan en forma de cocientes de intensidades entre las subcapas L y cocientes de intensidades entre transiciones particulares, ambos medidos con respecto al número total de fotones de rayos X registrados. Se realizaron microanálisis complementarios (AFM, SEM/EDS) con el propósito de obtener información certera acerca de la composición química y propiedades superficiales de las películas delgadas en regiones de interés determinadas.

Descriptores: PIXE; intensidad relativa de líneas de rayos X; física de Aceleradores de Baja Energía.

PACS: 29.20.Ba; 29.30.Kv; 81.40.Wx; 81.15.Dj.

1. Introduction

The use of charged particle beams like protons, alpha particles and other heavy ions from accelerators as a means of characteristic X-Ray production for non-destructive elemental analysis in a large variety of materials has been an important topic for Accelerator Physics over the last decades. In particular, it has been demonstrated along several years and a variety of applications that Particle Induced X-Ray Emission (PIXE) has great advantages over similar techniques, singular characteristics worth of mention are the great sensitivity for measuring element traces in a given sample, and the excellent ratio of X-ray production cross section to background bremsstrahlung contribution. PIXE has covered the growing need for a rapid non-destructive multi-elemental analysis technique, which probes the surface and near-surface region of materials in diverse fields such as, biological, environmental, geological, metallurgical, archaeological and materials sciences.

In general, PIXE analysis consists of two parts. First it is necessary to identify the atomic species in the target from the energies of the characteristic X-rays lines present in the X-ray emission spectrum; and then the second part consists in determining the amount of a particular element present in the target by using the intensity of its characteristic X-ray emission spectrum. Such procedure requires knowledge of the ionization cross sections, fluorescence yields, Coster-Kronig rates, absorption coefficients, and relative intensities, among other atomic parameters. For applications of the PIXE technique, as well as fundamental Atomic Physics of inner shell processes it would be ideal to have a complete description of the L-shell vacancy decay mechanisms, which can be only achieved by fully understanding all of the atomic parameters involved.

In this work we have performed an experimental study on the energy dependence of the characteristic X-ray lines relative intensities, which is one of the most important atomic parameters, since it is directly related to the X-Ray emission cross sections, but with the advantage that such intensities can be measured directly from experimental results, without having to involve more atomic parameters into calculations. Mainly, motivation for performing this kind of study comes from two sources: one is to provide a test ground for the different theoretical models currently used to calculate the intensity ratios of the characteristic X-ray lines; and the second and more ambitious is the possibility of developing an "upgrade" of PIXE, which could allow the technique to determine the chemical environment effects for a given element in an analytical spectra.

2. Experimental

In order to induce the emission of Gd characteristic X-rays, a proton beam was used. The charged particle beam was produced by means of a Van de Graaff accelerator, allowing us to have protons with energies between 200 keV and 750 keV. Details on the experimental procedure can be found in [1, 2]. In brief, once the beam is accelerated to the desired energy, an analyzing magnet deflects it and then enters the analysis chamber, where the sample is located forming a 45° angle

between the beam direction and the sample normal. Typical vacuum for the transport system and analysis chamber is on the order of 10^{-6} torr. Samples were in the form of thin films, with thicknesses of about 0.17 μm (measured by RBS) deposited onto pyrolytic Carbon substrates. Such films were produced by heating GdF_3 powder with a tungsten filament, until evaporation of GdF_3 was achieved. Emitted X-rays were recorded by means of a Canberra SL30165 Si(Li) detector, with a resolution of about 165 eV FWHM, the detector is outside the vacuum chamber, separated by a 4 μm thick Mylar window, and 3 cm away from the sample (most of this distance inside the vacuum chamber). Simultaneously, inside the chamber a Canberra PD-25-12-100 PIPS detector recorded backscattered particles. Finally, the PIXE and RBS spectra were collected in an Ortec MCB926 multichannel and the associated electronics. A typical PIXE spectrum of the GdF_3 sample is shown on Figure 1.

For each one of the selected bombardment energies both a PIXE and a RBS spectrum were generated. Since statistics on the weakest X-ray lines was an important factor for the analysis, the L_l line was used as a control for the spectra acquisition. At least 1000 raw counts in such line were acquired in order for the data to be recorded.

Since part of the studies we performed for this work involve establishing the viability of using the PIXE technique to characterize the chemical environment of a given element, it was necessary to perform complementary micro-analysis techniques in order to provide as much as possible information on the surface and near-surface features of the samples, with special interest in establishing if there was any differences on the films surface properties and elemental composition before and after irradiation. Such analyses were performed in a JEOL SEM-5600LV and JEOL SPM-4210 (AFM mode) microscopes. Regions corresponding to *"without irradiation"* and *"after irraditation"* on the GdF_3 sample are shown in Figure 2.

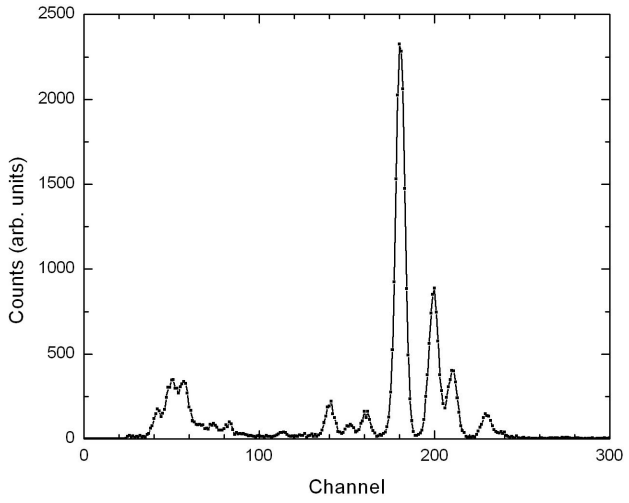

FIGURE 1. Typical X-ray spectrum of Gadolinium, emission of the characteristic X-rays is induced by 600 keV protons.

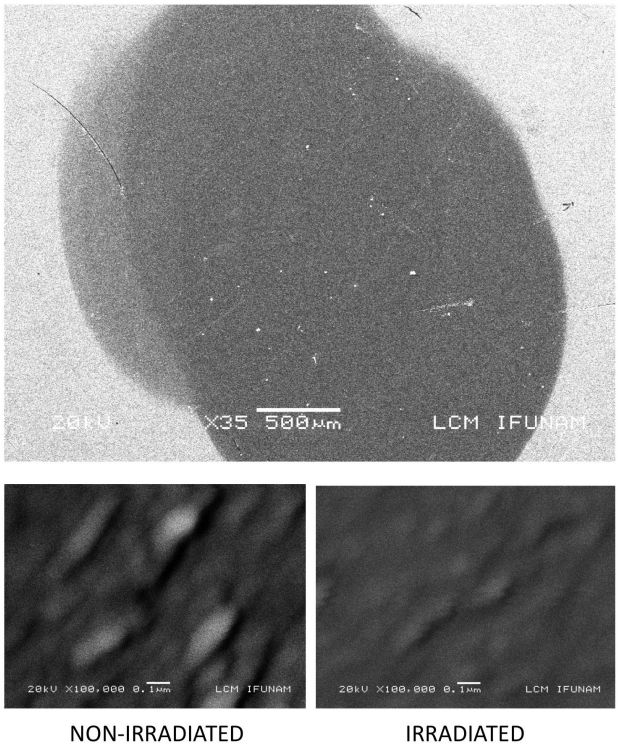

FIGURE 2. Top: SEM image of the surface of the sample, where the clear region corresponds to "non-irradiated" and the dark circular-shaped region is the corresponding to the region "irradiated" with protons. Bottom: Same as before, but with a higher zoom factor.

3. Analysis and results

3.1. PIXE analysis

In order to use the recorded X-ray spectra in further calculations, first it was necessary to calibrate the detector. To do so we followed the procedure described in detail in [3]. In brief, characteristic X-Rays induced by a 600 keV proton beam coming from calibrated targets manufactured by MicroMatter were used to measure the detector efficiency in the energy range used during the experiments, through a combination of the following equation and a fit to the experimental data obtained:

$$\varepsilon(E) = \frac{N_X \sigma_R(E_0)\Omega_R}{N_R \omega_K \sigma_K(E_0)} F(E_0) \qquad (1)$$

In this equation $N_X$is the number of photons recorded by the X-ray detector, N_R is the number of backscattered particles registered by the particle detector with a solid angle given byΩ_R, $\sigma_R, \sigma_K$are the cross sections for Rutherford backscattering and ionization of the K-shell respectively, ω_K is the fluorescence yield of the K-shell, and $F(E_0)$is a correction factor for X-ray self absorption and ion stopping in the emitting film [4]. Ionization cross sections were computed using the ISICS code [5] in the ECPSSR approximation, and Rutherford cross sections were calculated as in [6].

X-ray and RBS spectra for the calibrated targets were analyzed by means of the WINQXAS [7] and SIMNRA [8] computer codes respectively.

Once the X-ray detector is calibrated it is possible to analyze the set of X-ray spectra generated by the bombardment of the GdF_3 samples. Each one of the X-ray spectrum were analyzed using a combination of the WINQXAS and GUPIX [9] codes, which allowed us to have a more accurate deconvolution of the characteristic X-ray peaks, with the corresponding correction by the efficiency function and any absorption parameters involved. Experimental data was sorted in two different ways: first we measured all the X-ray peaks intensities and sum them, thus generating an L_{TOT}coefficient, then we choose only those peaks coming from a particular subshell, generating in the same way the intensities of each subshell (L_1, L_2, L_3), allowing us to calculate the following ratios:

$$R_i = \frac{L_i}{L_{TOT}} \quad (i = 1, 2, 3) \tag{2}$$

The other way for sorting the experimental data was considering individual peaks, which we could resolve in the X-ray spectra$(L_{\alpha 1}, L_{\beta 1}, L_{\beta 2}, L_{\gamma 1}, L_{\gamma 3}, L_l)$, and then we used that information for computing the ratios given as:

$$S_i = \frac{L_i}{L_{TOT}} \quad (i = \alpha_1, \beta_1, \beta_2, \gamma_1, \gamma_3, l) \tag{3}$$

Since this work is intended to be used as a basis for a further description of the phenomena studied, where not only protons but also heavier ions will be considered; we decided that description of the S_i ratios require an independent variable which could be used also for a variety of projectiles. For this purpose we define a *"reduced velocity"* (*VR*) as:

$$VR = \frac{v_p}{v_L} \tag{4}$$

Where v_p is the classical projectile velocity, and v_L corresponds to an average velocity of the electrons on the L-shell, defined as:

$$v_L = \frac{1}{4}\left(v_{L1} + v_{L2} + 2v_{L3}\right) \tag{5}$$

Results for the S_i ratios are presented in Figure 3. Also in this plot, calculations for the same ratios are shown, for both PWBA and ECPSSR approximations. In order to compare these calculations with the experimental data, we defined the theoretical $S_i^{(T)}$ratio as:

$$S_i^{(T)} = \frac{\sigma_{Li}^{eff}\omega_{Li}}{\sum_{i=1}^{3}\sigma_{Li}^{eff}\omega_{Li}} \quad (i = 1, 2, 3) \tag{6}$$

Where the ω_{Li} correspond to the fluorescence yield of each L sub-shell, and the effective cross sections $\left(\sigma_{Li}^{eff}\right)$ are calculated as follows:

$$\begin{aligned} \sigma_{L1}^{eff} &= \sigma_{L1} \\ \sigma_{L2}^{eff} &= \sigma_{L2} + f_{12}\sigma_{L2} \\ \sigma_{L3}^{eff} &= \sigma_{L3} + f_{23}\sigma_{L2} + (f_{13} + f_{12}f_{23} + f'_{13})\sigma_{L1} \end{aligned} \tag{7}$$

Where the coefficients f_{ij} correspond to Coster-Kronig transitions, and the cross sections (σ_{Li}) were calculated with the ISICS computer code. Atomic parameters employed for these calculations had the values [10, 11, 12]:

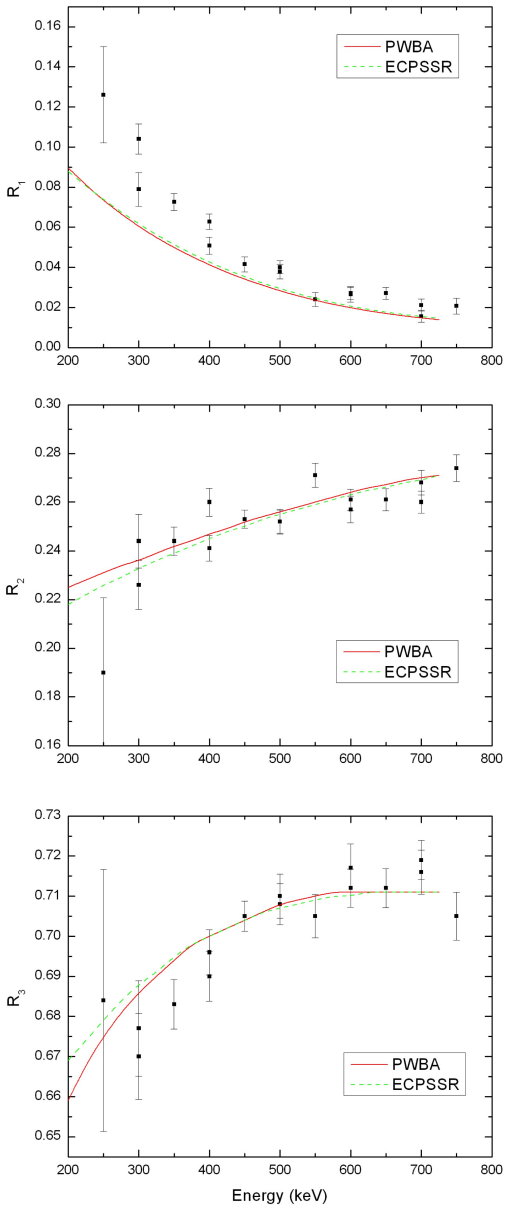

FIGURE 3. Intensity ratios Ri as a function of projectile energy. Solid line corresponds to PWBA approximation; dashed line corresponds to ECPSSR correction.

Fluorescence yields	$\omega_{L1} = 0.101,$
	$\omega_{L2} = 0.175,$
	$\omega_{L3} = 0.167;$
Coster-Kronig coefficients	$f_{12} = 0.166,$
	$f_{13} = 0.166,$
	$f'_{13} = 0.166,$
	$f_{23} = 0.147.$

Main features of the R_i ratios can be summarized as follows: a good agreement can be observed between experimental results and theoretical predictions; also, both approximations (PWBA and ECPSSR) agree, except for the region corresponding to low energy (about 300 keV) in the R_2 *and* R_3 ratios. Only the R_1 ratio exhibits a decreasing behavior, while the other two ratios (R_2, R_3) increase with the projectile energy. Main contribution to the uncertainties of the R_i ratios come from the statistics, for the lowest energies it was almost impossible to get as good statistics on the X-ray spectra as for the higher ones, due to the time required for recording the information during the experiments.

Some of the individual-peak ratios S_i are shown in Figure 4. In this case we did not perform any theoretical calculations, and we present only the experimental data. It has been possible, however, to compare the results generated during this work with previous measurements, which are not shown here. In a future publication, we will deal with the analysis of the cloud of experimental results, including our measurements and previous measurements, but for the main purpose of this work we will present only our data set. It is worth mentioning, however, that validity of our experiments has been crosschecked by comparing the R_i ratios with theoretical predictions, which could be considered as the integral information of all our measurements. And as we mentioned before, by comparing our results with previous measurements, including even different targets brought together by using the *VR* variable, it is possible to establish that they are in agreement.

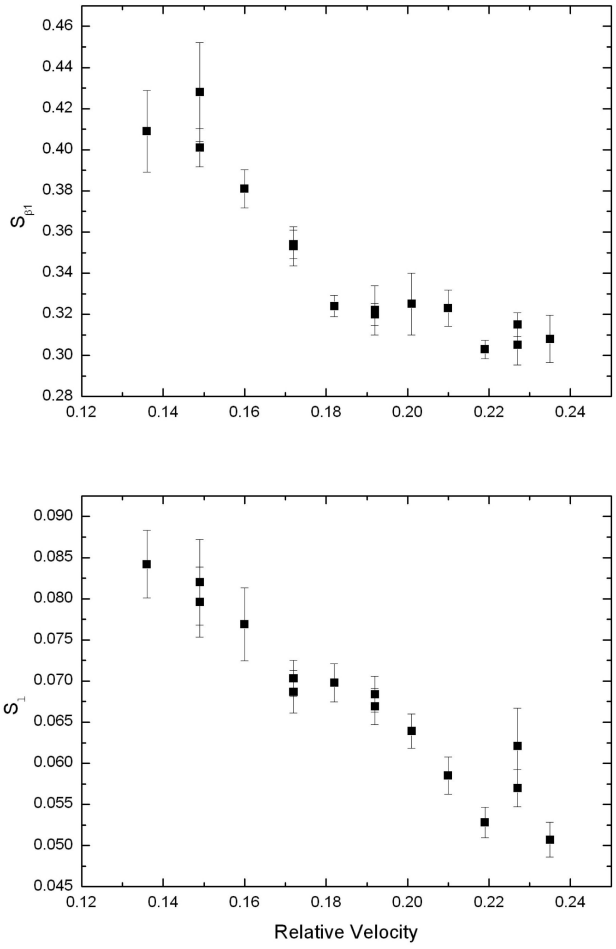

FIGURE 4. Intensity ratios $S_{\beta 1}, S_l$ as a function of Relative Velocity (VR).

3.2. Micro analysis

As we mentioned before, since the main target of this work is to establish the possibility of using PIXE as an analytical technique that provides not only elemental information, but also provides direct data on the chemical state or chemical environment in which the atoms corresponding to the element of interest are immersed. It is necessary to completely characterize the samples studied, which goes further away from the reach of the basic accelerator-based analysis techniques. For this reason we performed a series of complementary studies of the GdF_3 samples, consisting in Scanning Electron Mycroscopy with Energy Dispersive X-ray Spectroscopy (SEM/EDS) and Atomic Force Mycroscopy (AFM) studies. We focused these studies in establishing differences between the non-irradiated GdF_3 film, and the irradiated regions. As shown in Figure 2, it is straightforward (and even to the naked eye) to identify such regions on the film surface.

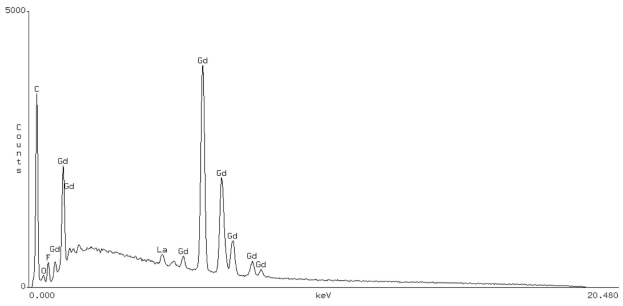

FIGURE 5. EDS spectrum of the sample, corresponding to a *"non-irradiated"* region.

Both microscopy techniques show the existence of a preferential direction for the growth of the films, which has been attributed to the combination of the evaporation technique and the substrate employed. A typical spectrum acquired by

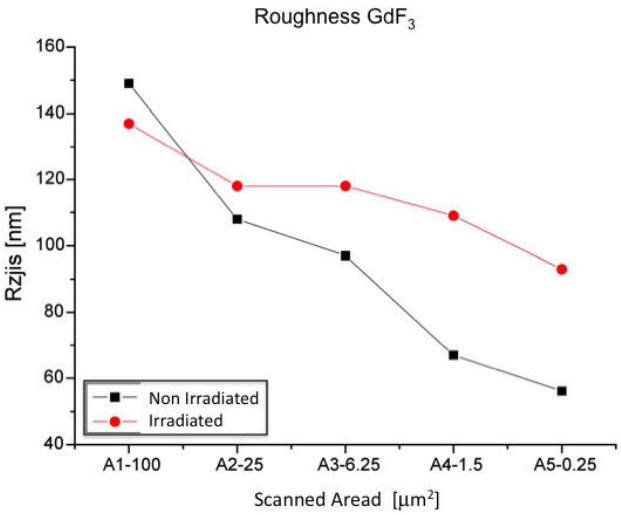

FIGURE 6. Results for the film surface roughness of the sample in Japanese Industrial Standard (JIS) units of R_Z. Measurement regions are indicated at the bottom of Figure 7.

EDS is shown in Figure 5, corresponding to non-irradiated regions of the film. A detailed analysis of the atomic percentages of the elements present in the sample indicates that the original stoichiometry of the GdF_3 was lost during the evaporation, giving place to a reactive Gadolinium surface, which associated with atmospheric oxygen, in the expected form of Gd_2O_3. It is only after this superficial Gd_2O_3 film was irradiated with protons, that Oxygen detaches the film. Atomic rates are shown in table I. Ideal concentrations correspond to GdF_3 and Gd_2O_3, experimental data shows that films were richer than expected in Gadolinium before and after irradiation, but only Oxygen disappears noticeably from the sample after irradiating this with protons. On the other hand, AFM provides accurate information on the surface roughness. This technique shows that the roughness of the sample increases on the irradiated regions (see Figure 6). However, grain profiles of the sample illustrate that the shape of such grains becomes *"softer"*, but still they remain attached to the substrate (see Figure 7). Thus, an interpretation of the experimental results lead to the fact that the grains, which are forming the film, become more uniform and with defined shapes but also more separated one from each other after the sample was irradiated with protons.

TABLE I. Rates of Gd/F and Gd/O measured from the atomic percentage concentration composition of the samples, and determined by SEM/EDS microscopy technique in regions non-irradiated and irradiated with protons during the experiments.

Rates	Ideal	Non-Irradiated	After Irradiation
Gd / F	0.33 (GdF_3)	3.95 (0.26)	3.58 (0.25)
Gd / O	0.66 (Gd_2O_3)	13.86 (0.58)	6.53 (0.45)

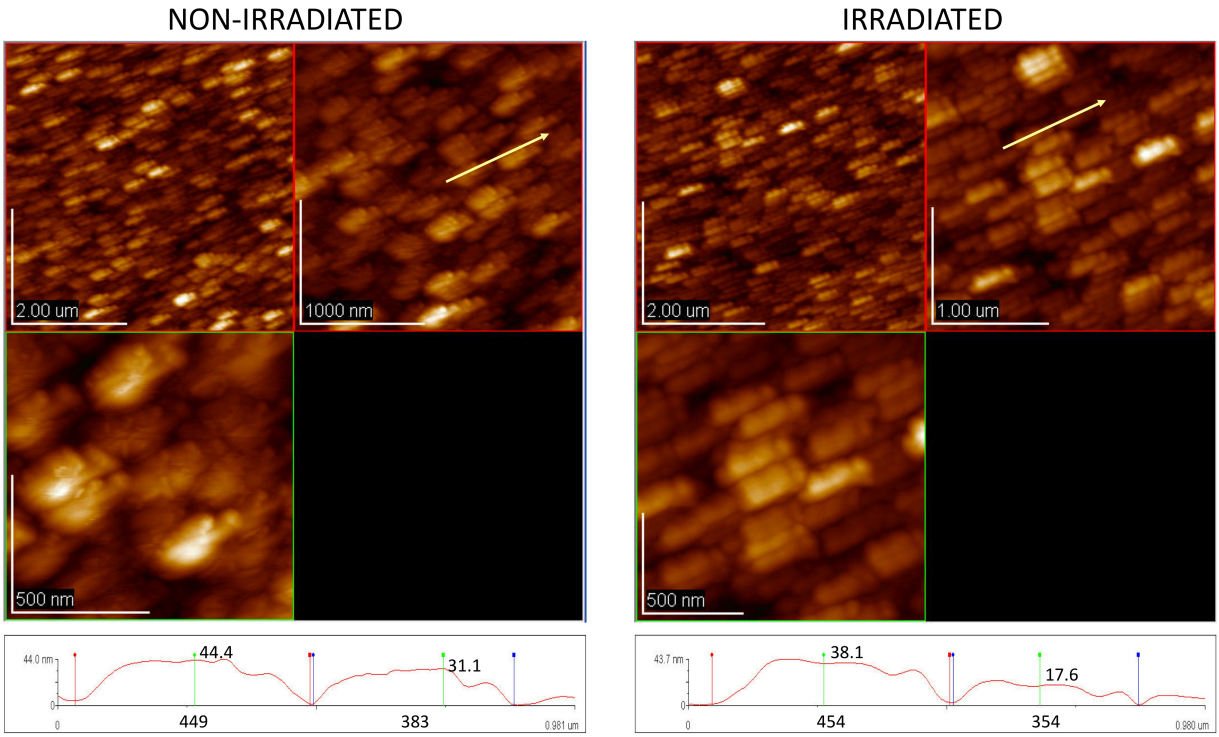

FIGURE 7. AFM images of the sample corresponding to different zoom factors. Bottom: regions and data used for measuring the surface roughness of the samples.

4. Remarks

In this work we presented relative intensities of Gadolinium characteristic L X-rays, induced by proton bombardment. Through the experimental data presented here we have established the existence of an energy dependence of such intensity ratios. In addition to the energy dependence we have introduced a variable, which will allow to compare different projectile-target systems, in order to perform a deeper analysis of the characteristic X-ray relative intensities, for any given element. Since the aim of this work includes an extension of the capabilities of the PIXE technique, which could provide direct information on the chemical environment in which the atom of interest is immersed, a series of microanalysis were performed. These analyses clearly indicate differences in the stoichiometry and surface properties of the samples induced by the proton irradiation and even the procedure for producing the thin films.

Acknowledgements

This work was partially supported by UNAM-PAPIIT under contract number IN-105510.

The authors acknowledge the technical work of J. Cañetas, D. A. Quiterio, and M. Galindo.

1. J. Miranda, R. Ledesma. O. G. de Lucio, *App. Rad. and Isot.* **54** (2001) 455.
2. J. Miranda, O. G. de Lucio, E. B. Téllez, J. N. Martínez, *Rad. Phys. Chem*. **69** (2004) 257.
3. O. G de Lucio, J. Miranda and L. Rodríguez-Fernández. *Rad. Phys. Chem*. **73** (2005) 189.
4. J. Braziewicz, J.Semaniak, T. Cziwzewski, L. Glowacka, M. Jaskola, M. Haller, R. Karschnik, W. Kretschner, D. Trautmann, *J. Phys. B* **27** (1994.) 1535.
5. Z. Liu and S. Cipolla. *Computer Phys. Comm.*, **97** (1996) 315.
6. J. R. Bird and J. S. Williams, *Ion Beams for Materials Analysis*, (Academic Press, San Diego, 1988).
7. V. Van Espen, H. Nullens, F. Adams, *Nucl. Instr. And Meth. B* **142** (1977) 243.
8. M. Mayer, *SIMNRA User Guide Technical Report*, IPP 9/113 (Max Plank Institut Für Plamsmaphysik, Garching Germany).
9. J. L. Campbell, N. I. Boyd, N. Grassi, P. Bonnick, J. A. Maxwell, *Nucl. Instr. and Meth. B* **268** (2010) 3356.
10. W.T. Elam, B.D. Ravel, J.R. Sieber, *Rad. Phys. Chem*. **63** (2002) 121.
11. O. G. de Lucio and J. Miranda, *Nucl. Instr. and Meth. B* **248** (2006) 47, and references cited therein.
12. O. G. de Lucio, J. Miranda, *Rev. Mex. Fis* **50** (2004) 319, and references cited therein.